15th International Conference on Fluid Control, Measurements and Visualization
27-30 May 2019, Naples, Italy

Analysis for the fastest streamlined posture of swimmers

Soki Imamura[1], Shinichiro Ito[2,*] and Masaki Hiratsuka[2]

[1]Department of Mechanical Engineering, Graduate School of Kogakuin University, Tokyo, Japan
[2]Department of Mechanical Engineering, Kogakuin University, Tokyo, Japan
*corresponding author: ito@cc.kogakuin.ac.jp

Abstract Competitive swimming is a sport that competes for speed. It is divided into two aspects. The one is a glide aspect as the start and turns phase and the other is a stroke aspect as constant speed motion phase accompanied by movement of hands and legs in a race. The glide phase is the fastest speed during the competition and leads to time shortening. It is important to take a posture with low propulsive drag. It is essential for the swimmer to keep deceleration suppressed by keeping the low pressure drag, while buoyancy and lift due to the posture is balanced with the self-weight, and maintaining fast speed to connect the stroke phase. The purpose of this research is to propose a streamlined posture that can swim with maintaining a certain depth and has less drag. In this study, CFD analysis was performed on 14 cases of streamlined posture with the altered angle of attack of each arms body, and leg to grasp its buoyancy and drag. In order to confirm these results, aerodynamic experiments were performed on models with the same shape used in the calculation in wind tunnel. The calculated results also agreed well with the wind tunnel experiment results.
Keywords: CFD, streamline posture, neutral buoyancy

1 Introduction

In swimming, it is important to reduce drag to swim faster. The streamline is a common ability evaluation standard from beginners to experts. It cannot get the momentum such as stroke or kick. However, the improvement of the streamline posture is directly linked to the rapid promotion by drag reduction especially at the start and turn phase. Ando et al. [1] reported that when a complex shape such as the human body moved in water, the flow behind the back of the head and buttocks was separated downstream and a negative pressure was generated, even in horizontal posture. The flow separation creates pressure drag. Havriluk [2] reported the passive drag of level swimming and that faster swimmers had a significantly lower coefficient of drag (Cd) than slower swimmers. Bixler [3] determined the accuracy of using CFD for the analysis of the hydrodynamics of swimming and the drag forces calculated from the virtual model using CFD were found to be within 4% of the experimentally determined values for the mannequin. Thus, the streamline posture is important for swimming faster. Deep dives greatly reduce the wave resistance [4]. Maintaining depth and reducing pressure resistance leads to record updates. Similarly, CFD regarding swimming is being performed [5, 6]. The purpose of this research is to find a streamline posture with low drag under the condition that the lift and the weight of the downward force are in balance in order to keep the depth constant.
A streamline posture was created by 3D CAD, and flow analysis around streamline posture was performed. In addition, a streamline model was created using a 3D printer, and wind tunnel experiments were conducted to compare with the CFD results, and the validity of the calculation was confirmed.

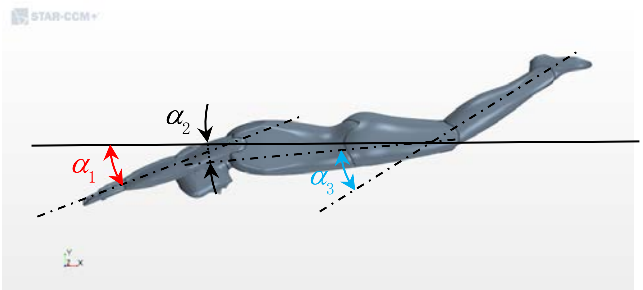

Fig. 1 Streamline posture and the definition of angle of attack concerning arms, torso and legs.

2 Method

2.1 Numerical Analysis

2.1.1 Streamline posture to be analyzed Streamline postures were created using the 3D-CAD software SOLIDWORKS. Figure 1 shows the streamline postures and the absolute angles of attack on the uniform flow of the arms, torso and legs. Table 1 shows the posture names Case1 to Case14 defined by each angle of attack.

Table 1 Outline of streamlines

Case #	Streamline #	Arm angle, α_1	Torso angle, α_2	Leg angle, α_3
1	Streamline 1	0°	0°	0°
2		10°	10°	10°
3	Streamline 2	15°	0°	30°
4		21°	10°	36°
5		25°	10°	40°
6	Streamline 3	15°	0°	0°
7		25°	10°	10°
8	Streamline 4	0°	0°	30°
9		10°	10°	40°
10	Streamline 5	15°	0°	15°
11		21°	6°	21°
12		25°	10°	25°
13	Streamline 6	0°	0°	15°
14		10°	10°	25°

2.1.2 Analysis method The computational grid shown in Fig. 2 was created by mesh operation of the fluid space. The outer periphery was a polyhedral mesh with a standard size of 0.2 m and was set to become finer as it approached a streamline model with a total length of 2.4 m. As shown in Fig. 3, the mesh around the streamline model has a boundary layer thickness of 0.01 m, and It is composed of 10 prism layer meshes, and the thickness increases exponentially from the bottom layer thickness, 0.003 m.
The analysis region shown in Fig. 4 was a fluid region with a depth of 3.0 m, a width of 3.0 m, and a length of 15.0 m. The main boundary conditions in the fluid region were the velocity boundary at the head side inlet wall, the pressure boundary at the toe side outlet, the object and the other surface were the wall boundary as shown in Table 2. In addition, the inlet velocity was defined as U = 3.1 m / s corresponding to the international swimming level at the start and turn phase, temperature was assumed to be 298 K, and the density and viscosity at this temperature are set as shown in Table 3. The fluid analysis was performed in these conditions.

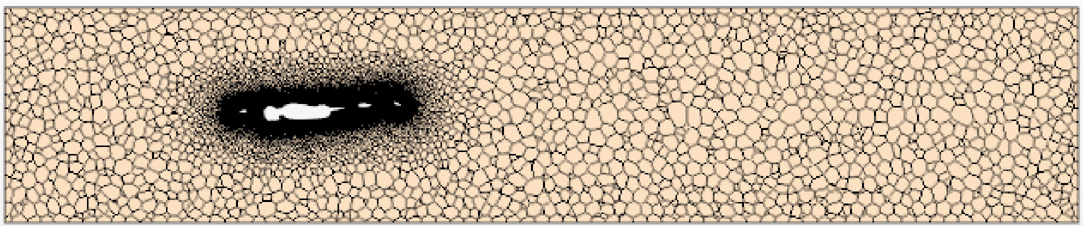

Fig 2 Computational grid of whole calculation area

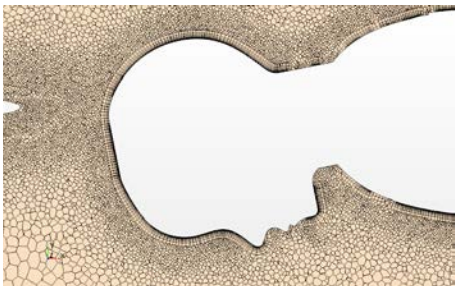

Fig 3 Computational grid around a streamline model

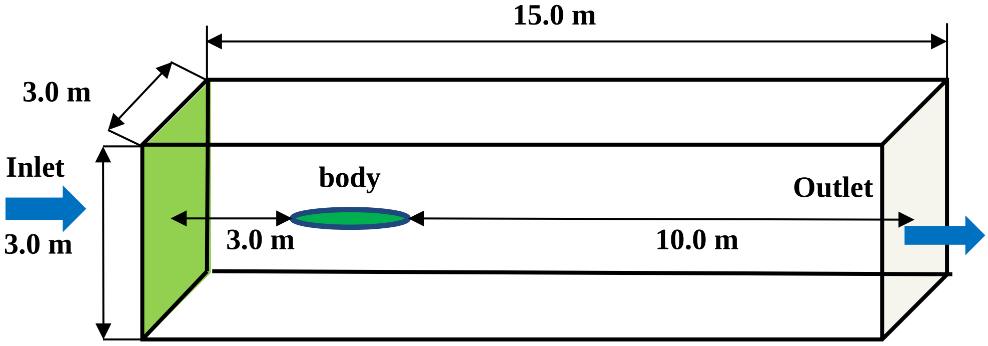

Fig 4 Analysis area

Table 2 Boundary condition

Boundary	Boundary condition
Inlet	Speed inlet 3.1[m/s]
Outlet	Pressure outlet
Body	Wall
Other surface	Wall

Table 3 Physical properties

Density of water ρ [kg/m^3]	997
Kinetic viscosity ν [m^2/s]	8.93×10^{-4}
Body length (1.8m) with arm[m]	2.4
Swimming velocity [m/s]	3.1
Reynolds number	6.23×10^{6}

2.1.3 Analysis condition The analysis conditions were up to 1,000 times of calculation until the residual converges. The discretization of the equation uses the finite volume method, and the governing equation is the Reynolds average Navier-Stokes equation. The analysis conditions were set in the *k-ε* turbulence model as three-dimensional steady state analysis, liquid, separated flow, and turbulent flow.

2.2 Experiment

Models of the same postures as the calculation were created using a 3D printer for wind tunnel experiments as shown in Table 4. Each posture is the basic streamline shown in Table 1, and 14 cases could be represented by changing the attack angle of the torso. The length of models of Streamline 1 were 0.465 m. In order to make the flow field on the model surface turbulent, 0.2 mm blast sand was sprayed on the model surface like Fig 5, and each fluid force was measured at 30 m/s, i.e. Re=7.54×10^{6} in a wind tunnel. As shown in Fig. 6, the support rod connecting the model to the load cell was covered with the airfoil case to eliminate the influence of the fluid force of the support rod, and each fluid force of model was obtained accurately by removing the fluid force of the sting that supported the model separately.

Table 4 Fabricated models by 3D printer

	
Streamline 1	Streamline 2
	
Streamline 3	Streamline 4
	
Streamline 5	Streamline 6

Fig. 5 Streamline model with sand blasted

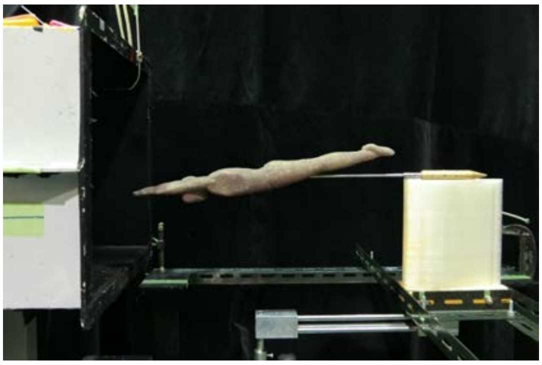

Fig. 6 Side view of the experimental landscape (Case2, 10° torso inclined)

3 Result and Discussion

3.1 Numerical Analysis

Figure 7 shows the difference in lift and drag due to each case in Table 1. Due to the weight and buoyancy of this size of swimmers, the downward lift 150 N is a neutral buoyancy that maintains a certain depth. The low drag postures with this condition should be excellent streamline postures for competitive swimming. Case 1 with the smallest drag had a negative lift or buoyancy. Therefore, it cannot maintain a constant depth. That is, it floats on the surface of the water gradually at the start and turn, and the swimmer receives a wave drag and slows down. On the contrary, if there is too much positive lift, the swimmer continues to dive deeply and does not receive wave drag, but the speed of the swimmer will fall because of the large pressure drag. Case 12 and Case 14 are the candidates for the neutral buoyancy around 150 N, but Case 14 with low drag is the optimum posture and attack angle. The causes of differences in lift and drag will be discussed below through pressure distribution maps for the characteristic postures.

We compare Case 1 which is a general streamline posture with Case 2 where the angle of attack is set to 10° on Case 1. Table 5 shows pressure distribution maps of Case 1 and Case 2 respectively. Case 2 with the angle of attack had higher back pressure and lower abdominal pressure than Case 1. Therefore, it was thought that the lift direction was acting in the downward. Despite the front projection area increased compared Case 1 with Case 2, the increase of drag was small. Figure 8 shows the path lines of Case1. Longitudinal vortices like tip vortices were observed at the toes, and the occurrence of drag from the feet was confirmed. It was found that the foot posture was important for reducing drag.

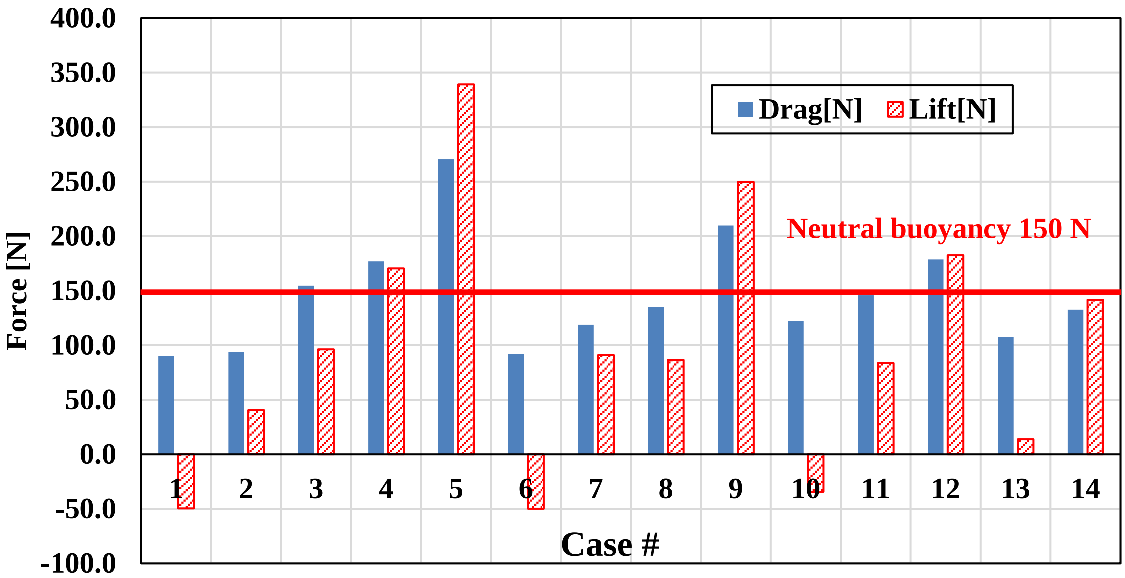

Fig. 7 Calculation result of lift and drag for each case

Table 5 Influence of angle of attack on whole body

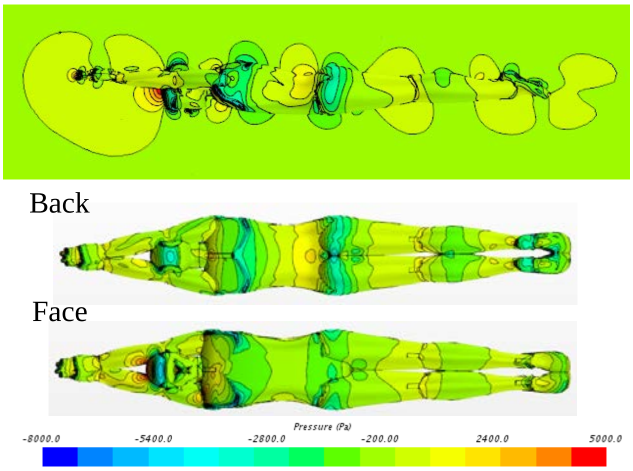	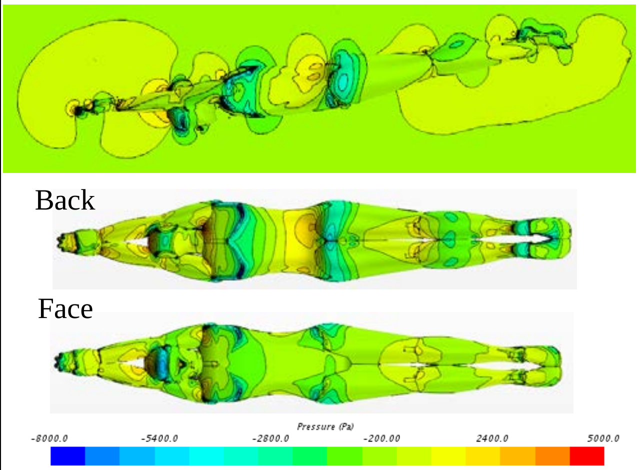
Pressure distribution map of Case1	Pressure distribution map of Case 2

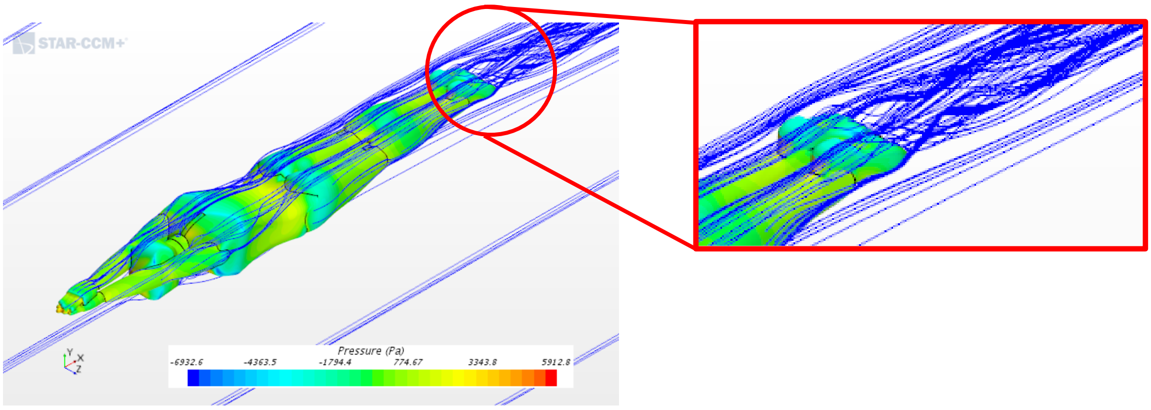

Fig. 8 Streamline of wing tip vortex generated from foot in Case 1

Table 6 compares Case 1 with Case 6 in order to confirm the effect of angle of attack on arms. Although there is a subtle difference in pressure distribution, it was found that the angle of attack of the arm was less effective on lift and drag.

Table 6 Influence of angle of attack on arms

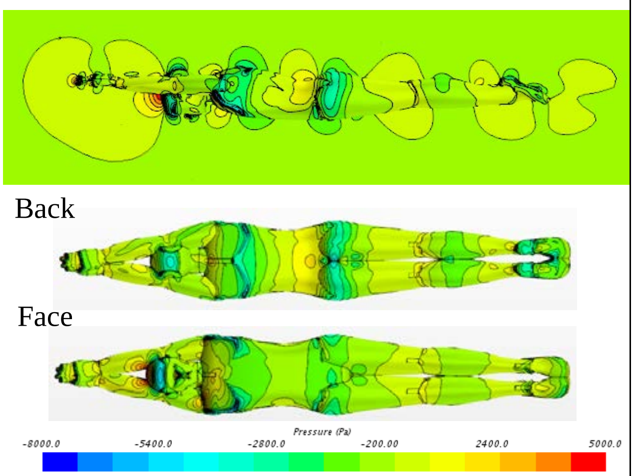	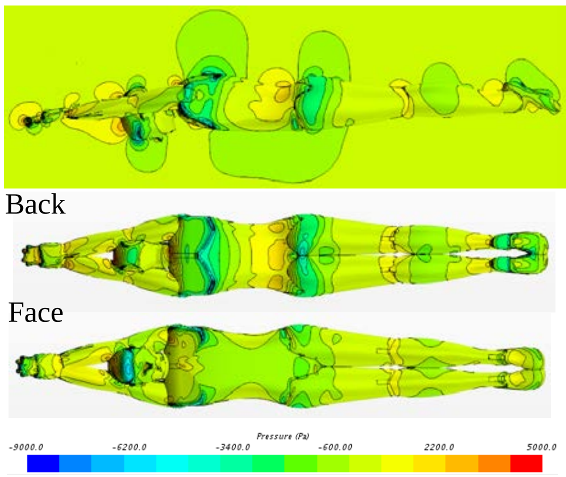
Pressure distribution map of Case 1	Pressure distribution map of Case 6

Table 7 confirms the effect of knee bending. By bending the knee, a difference in pressure distribution can be seen near the knee. It was found that bending the knee is more effective for increasing the downward lift than lowering the arm. However, as the front projection area increased, the drag also increased.

Table 7 Influence of angle of attack on legs

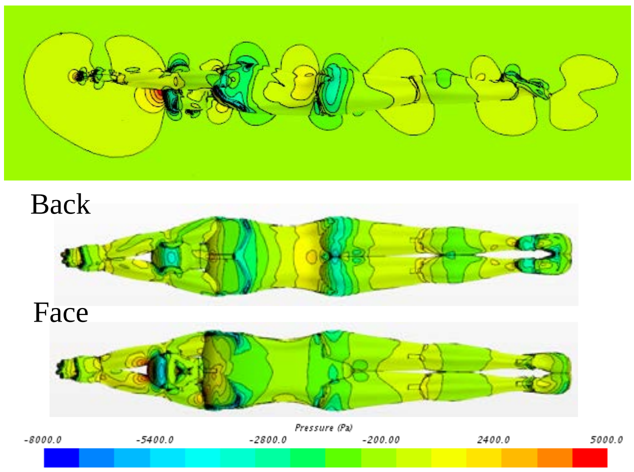	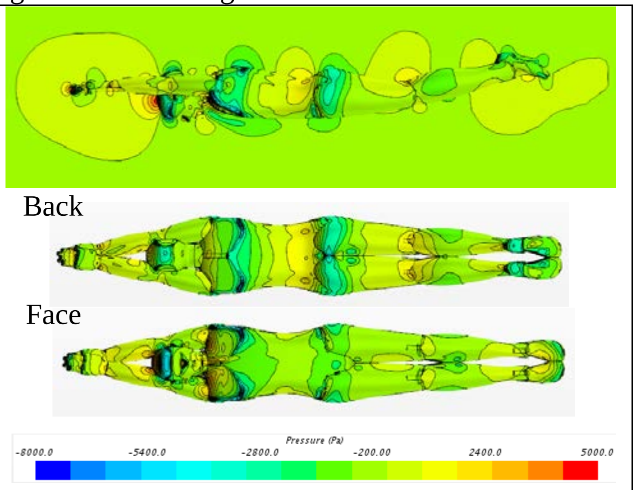
Pressure distribution map of Case 1	Pressure distribution map of Case 8

Next, we compare Case12 and Case14, which have values close to the neutral buoyancy (150 [N]) shown in Table 8. These two are candidates for competitive swimming streamline posture. Case12 and Case14 had a large pressure difference between the back and front part as a whole. The downward lift was affected by the angle of attack of the torso portion as well as the posture to bend the knee and to lower the arm. Both lift and drag increased due to the pressure difference between the top and bottom. But compared with the other cases, the change of attack angle from the body attack angle to the knee was appropriate. Therefore, the leg part was thought not to reach flow separation and gained lift.

Table 8 Top two streamline posture

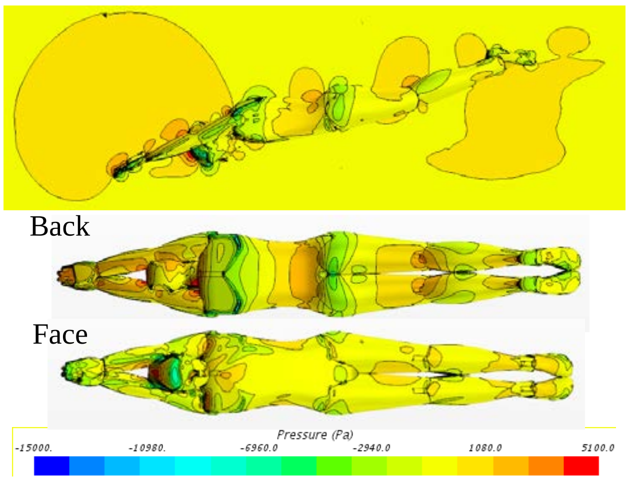	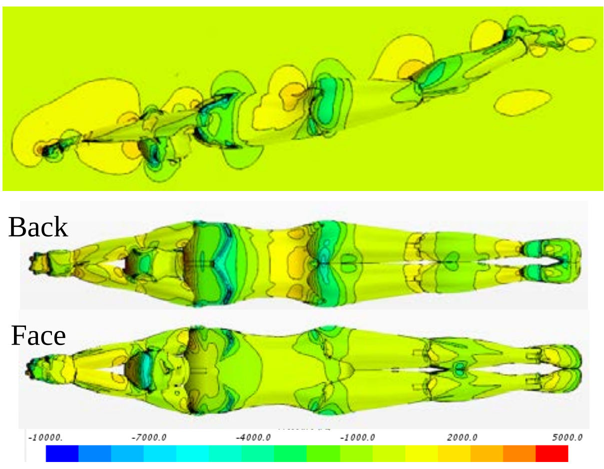
Pressure distribution map of Case 12	Pressure distribution map of Case 14

3.2 Experiment

Figures 9 and 10 show the results of comparing the drag coefficient C_D and the lift coefficient C_L for the experiment (Re=7.54×10^5) and Numerical Calculation (Re=6.23×10^6) in each case, respectively. The downward lift is defined as positive. Regarding C_D on the experiment, the turbulent boundary layer was developed because blast sand was applied to the surface of the experimental model. Therefore, the average error from the experimental value was 4.6% based on the calculated value. However, C_L had a large difference, with an error of 46%. The influence of Re can be considered for the fact that the lift coefficient does not match with the result of the calculation.

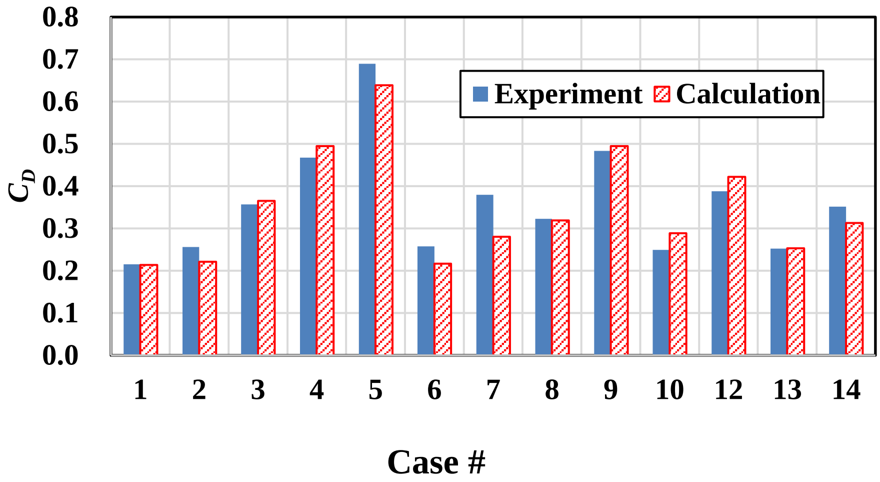

Fig. 9 Comparison between experiment and calculation on Drag coefficient, C_D

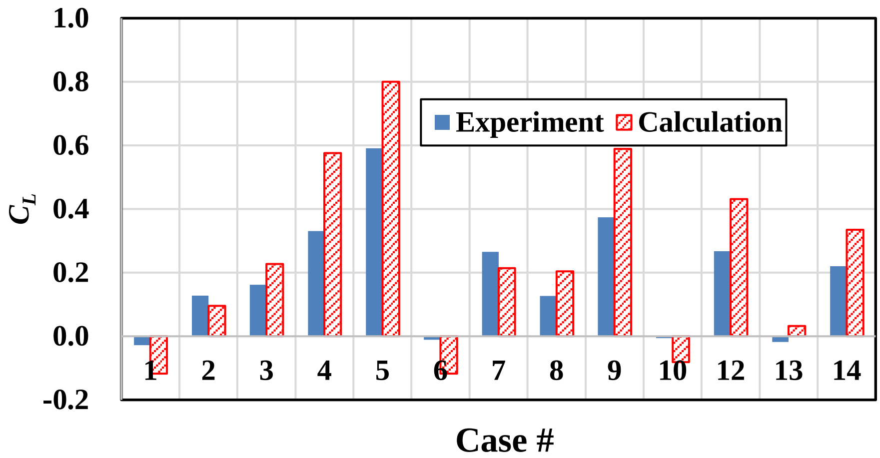

Fig. 10 Comparison between experiment and calculation on Lift coefficient, C_L

It was possible to be effective on the boundary layer with blast sand application, but it may not have been able to change the flow aspect. As a tendency, it can be said that Case12 and Case14 are the optimal streamline posture for the fastest start and turn also in experimental results.

4 Conclusions

In order to reduce the wave drag, we used CFD to estimate the streamline posture at the start and turn in the competitive swimming, which maintains a constant depth and a low drag, with the neutral buoyancy. The experimental models of the same shape in calculations were created and the validity of the calculation results was verified. In the case of C_D, the calculation was in good agreement with the experiment, and in the case of C_L, the same tendency of the experiment was found as in the calculation. The following conclusions can be drawn from the above results.

1) It was found that the lift and drag can be changed by bending the knee rather than lowering the arm.
2) By changing the angle of attack of the torso, the lift and drag are significantly changed.
3) The least drag streamline posture was Case 1, but it is not preferable because it has buoyancy.
4) The neutral buoyancy was obtained in Case 12 and Case 14, and the posture with less drag was Case14.

References

[1] Ando, K., Sengoku, Y., Tsubakimoto, S. (2013), Effects of Head Position Differences on Streamlined Posture in Swimming Performance, Bull. faculty. Health & Sci, Univ. of Tsukuba 36, 133-136 (in Japanese).
[2] Havriluk, Rod (2005), Performance Level Differences in Swimming, J. Research Quarterly for Exercise and Sport, 76-2, 112-118.
[3] Barry Bixler, David Pease, Fiona Fairhurst (2007), The accuracy of computational fluid dynamics analysis of the passive drag of a male swimmer, J. Sports Biomechanics, 6-1, 81-98.
[4] RossVennell, DavePease, BarryWilson (2006), Wave drag on human swimmers, J. Biomechanics, 39-4, 664-671.
[5] H. Zaidi, R. Taiar, S. Fohanno, G. Polodori (2008), Analysis of the effect of swimmer's head position on swimming performance using computational fluid dynamics, Journal of Biomechanics 41, 1350-1358.
[6] C.V. Popa, H. Zaidi, A. Arfaoui, G. Polodori, R. Taiar, S. Fohanno (2011), Analysis of w all shear stress around a competitive swimmer using 3D Navier–Stokes equations in CFD, Act of Bioengineering and Biomechanics Vol. 13, No. 1, 3-11.